

# Top-down measurements of contact resistivity.

Bart van Pelt

March 15, 2022

## Contents

<b>1</b>	<b>Introduction</b>	<b>2</b>
<b>2</b>	<b>Background</b>	<b>3</b>
2.1	Contact resistivity . . . . .	3
2.2	Typical measurement methods . . . . .	3
2.2.1	Cox and Strack . . . . .	4
2.2.2	Transmission line method . . . . .	5
2.2.3	Cross bridge Kelvin resistor . . . . .	5
2.2.4	Pin to plate . . . . .	7
<b>3</b>	<b>Theory</b>	<b>7</b>
3.1	A generalization: Transfer length effects . . . . .	7
3.1.1	Governing equations . . . . .	7
3.1.2	Uniqueness of solutions . . . . .	10
3.1.3	Influence of transfer length . . . . .	11
3.2	Idea: reduce effective sample dimensions . . . . .	11
3.2.1	TODOS . . . . .	14
<b>4</b>	<b>New approach</b>	<b>14</b>
<b>5</b>	<b>Characterization of measurement method</b>	<b>17</b>
5.1	TODOS . . . . .	19
5.1.1	<b>DONE</b> Why check validity/reliability? . . . . .	19
5.1.2	<b>TODO</b> How will I check if the method works? . . . . .	19
<b>6</b>	<b>Results</b>	<b>20</b>
6.1	Reliability . . . . .	20
6.1.1	TODOS . . . . .	21
6.2	Validity: Cross Bridge Kelvin Resistor comparison . . . . .	24

<b>7</b>	<b>Conclusion and outlook</b>	<b>25</b>
7.1	TODOS	25
7.1.1	<b>TODO</b> Ease of measurement	25
7.1.2	<b>TODO</b> Reliability of results	25
<b>8</b>	<b>Conclusion</b>	<b>25</b>
<b>9</b>	<b>TODO :noexport:</b>	<b>25</b>
9.1	<b>DONE</b> Waarde $L_t$ is ingeschat, wat betekent dit?	25
9.2	<b>DONE</b> Leuk, maar wat kunnen we hiermee?	25
9.3	<b>DONE</b> Implementatie: PCBs	25
9.4	<b>DONE</b> resultaten	25
9.5	<b>TODO</b> Reflectie	26
9.6	<b>TODO</b> Conclusie	26

## 1 Introduction

In the previous part of this thesis, the contact resistivity of Al-doped zinc-oxide on doped silicon was investigated, while omitting details on the performed measurements. In this part of this thesis, the devised measurement setup and method will be described in full detail. The method provides an alternative to typical contact resistivity measurements, in which several processing steps are needed to create accurately shaped contacts on the samples of interest. These methods include the Cox and Strack (C&S) and Transmission Line Method (TLM) methods, which will be explained later. Not only are these steps time-consuming and complicated to perform, they pose limitations on the types of samples that can be used. Furthermore, thermal and chemical processing steps could alter the electrical properties of the contact of interest, and there is no guarantee that the tested contacts accurately resemble the contact as it would behave in a practical device. At the start of this project a simple measurement method was suggested, coat a sample with a thin film of silver, drive a current between the top and bottom of this sample and measure the resulting potential difference. Multiplying the obtained resistance by the area of the sample should then give the specific resistance of the sample. While this suggested pin-to-plate measurement is very easy to perform, not needing any patterning and etching steps as required by C&S and TLM, it quickly became clear that the method was so unreliable that useful data could not be obtained. As the C&S and TLM methods provide some significant challenges, the choice was made to look deeper into the pin-to-plate method, and see if it can be improved on

enough to be useful. This work presents a solution to this problem, in which custom printed circuit boards are used to control the current flow in the samples. With this controlled current flow

The method devised here is able to characterize samples without the need of these patterning steps, requiring only a metallization step to ensure good contacts between the probes and the sample.

## 2 Background

### 2.1 Contact resistivity

Contacts between different materials often exhibit a voltage drop when a current is applied. In general, the relation between voltage drop,  $V$ , and resulting current density,  $J$ , can be described as

$$J = f(V, \text{other parameters}). \quad (1)$$

The other parameters may include, for example, the potential barrier height and doping densities of either material, their roles will be discussed later.

The contact resistivity is then defined as

$$\rho_c = \left. \frac{\partial V}{\partial J} \right|_{V=0}, \quad (2)$$

in which the dependency on the “other parameters” is implicit.

### 2.2 Typical measurement methods

Hier wil ik eigenlijk een beetje terugpakken op hoofdstuk drie van Semiconductor material and device characterization van Schroder. Het lijkt me een goed idee om van de two-terminal methods een paar te kiezen, zoals transmission line method en Cox & Strack, hoewel er andere varianten bestaan hebben ze allemaal hetzelfde praktische probleem: patterning stappen. Eigenlijk is de boodschap vooral “two terminal kan, maar je moet sowieso patternen, en interne weerstanden in je meetopstelling kunnen belangrijk zijn”. Daarna wil ik snel door naar de four terminal methodes. Hoofdzakelijk de cross bridge Kelvin resistor (CBKR) setup, maar ook even refereren naar alternatieve opstellingen (Loh et al. - 1985 - 2-D Simulations for accurate extraction ...). Belangrijke takeaway is hier het belang van de transfer length, en dat zaken makkelijker worden als deze groot is. Ook belangrijk om het voornaamste probleem te highlighten: scheiding van  $\rho_c$  en andere termen kan lastig zijn.

### 2.2.1 Cox and Strack

In the Cox and Strack (C&S) method samples are made that feature circular contacts of varying size on one side of the sample, while the other side has a full backplane contact, as illustrated in Figure 1. The resistance between

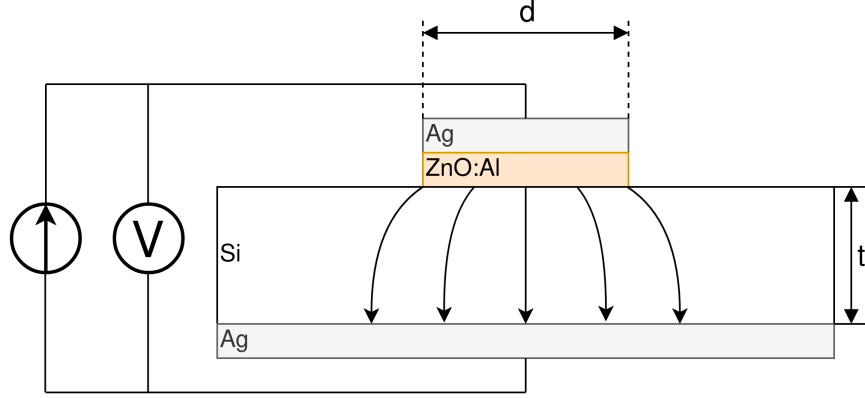


Figure 1: Illustration of a Cox and Strack measurement setup, the ZnO:Al and covering Ag layers are circularly shaped with diameter  $d$ , the Si and bottom Ag layers are much larger than the circular contact.  $t$  indicates the thickness of the Si layer. In practice, a single sample would be covered by multiple dots of varying diameter. The spreading resistance in the silicon scales differently with  $d$  than the contact resistance does, so that it can be fit out with sufficient data points.

the backplane and the circular contacts is then measured for the different circular contacts. The main assumption here is that the total resistance can be described as a sum of three resistances: contact resistance  $R_c$ , spreading resistance  $R_s$ , and some fixed residual resistance  $R_0$ . Cox and Strack model these terms as

$$R_T \approx \underbrace{\frac{\rho_W}{\pi d} \arctan\left(\frac{4t}{d}\right)}_{R_s} + \underbrace{\frac{\rho_c}{\frac{1}{4}\pi d^2}}_{R_c} + R_0, \quad (3)$$

where  $d$  is the diameter of the contact,  $\rho_W$  is the wafer resistivity,  $\rho_c$  the contact resistivity and  $t$  is the thickness of the wafer.

Since the contact and spreading resistances depend differently on the contact radius, the contact resistivity can be determined by varying  $d$  and fitting to the model. The practical implications of this method are that samples have to be precisely made, the circular contacts are typically tens of micrometers in radius. To make structures like this one would need to remove part of the contacting layer, for the delicate ZnO:Al films considered in this

work this is known to be difficult. Not only are these extra processing steps difficult to perform, they are incompatible with typical solar cell processes, so the question remains whether the fabricated samples accurately resemble the films in solar cell processes.

### 2.2.2 Transmission line method

The transmission line method (TLM) somewhat resembles the C&S method in the sense that multiple sample geometries are used to fit out the contact resistivity. In TLM, the chosen geometry is typically linear, with rectangular contacts spaced at different distances, as illustrated in Figure 2. Here again,

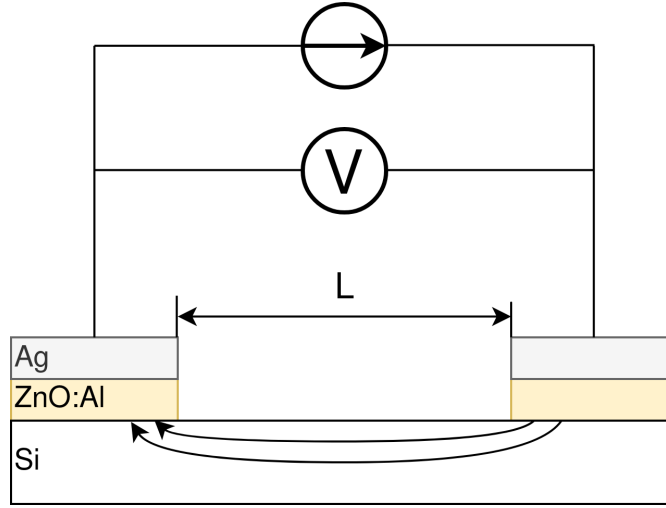


Figure 2: TODO

the resistances are measured for the different distances, and the contact resistivity can be fitted out.

The drawbacks here are similar to those in the C&S method, patterning and etching steps are required, making TLM not only difficult, but also possibly undermining the validity of the obtained results.

### 2.2.3 Cross bridge Kelvin resistor

While the previously described methods rely on being able to fit out the contact resistivity from some set of measurements, the cross bridge Kelvin resistor (CBKR) method takes a different approach. In essence the method is a top-down four-terminal measurement, a current is driven from the top

to the bottom of a sample using two terminals, while two other terminals are used to measure the resulting voltage.

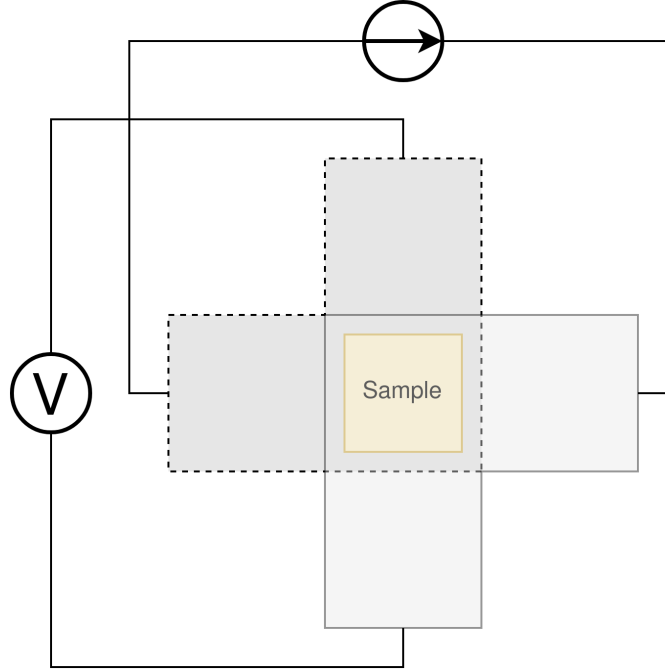


Figure 3: TODO

These electrodes are formed as two L-shapes, one on either side of the sample, with the “legs” opposed to each other. One set of opposed legs is used to drive the current, while the other opposed set is used to measure the voltage.

After measuring compute the total resistance of the sample, and multiply this by its area to get its specific resistance. With this approach parasitic resistances are easily ignored, as the voltage measuring wires carry no current. While the method might sound very simple, just drive a current and measure *the* voltage, a possible challenge lies in the basic assumption that the current is evenly distributed over the sample, or equivalently, that the contacting electrodes form isopotentials. When measuring samples with low specific resistivities these assumptions might not hold, currents can be localized near the edge of the sample, and the measured voltage might not accurately represent the average voltage across the sample. Additionally, misaligned contacts can result in currents “wrapping around” the sample, resulting in more systematic errors. In practice this results in a need for

well-controlled samples and a good understanding of the driven current distributions.

#### 2.2.4 Pin to plate

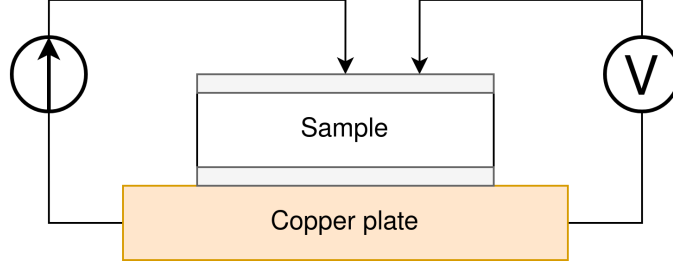


Figure 4: TODO

### 3 Theory

#### 3.1 A generalization: Transfer length effects

So far, all the top-down measurement methods had to mitigate one phenomenon, transfer length effects. Consider ideal conductors used as contacts, as these form regions of equal electric potential, the potential difference between top and bottom of the sample will be equal everywhere. The driven current density will be uniform, found simply by:  $J = \frac{\Delta V}{\rho_s}$ . In this idealized case, contact resistivities would be trivial to measure, but in reality the driven current distributions and potential differences can be significantly inhomogeneous, as illustrated in Figure 5. To quantify these effects, the interaction between electrodes and sample was modeled, as illustrated in Figure 6.

##### 3.1.1 Governing equations

In this model an arbitrary slab of sample and electrodes is considered, oriented along the x-y plane, with the z-direction defining the top and bottom of the setup. The electrodes are considered to be very thin, and relatively conductive, so that the voltage within each electrode are independent of  $z$ . Within these electrodes, the current density is determined by Ohm's law, so that

$$\vec{J}_{top} = -\sigma \nabla_{(x,y)} V_{top}(x, y), \quad (4)$$

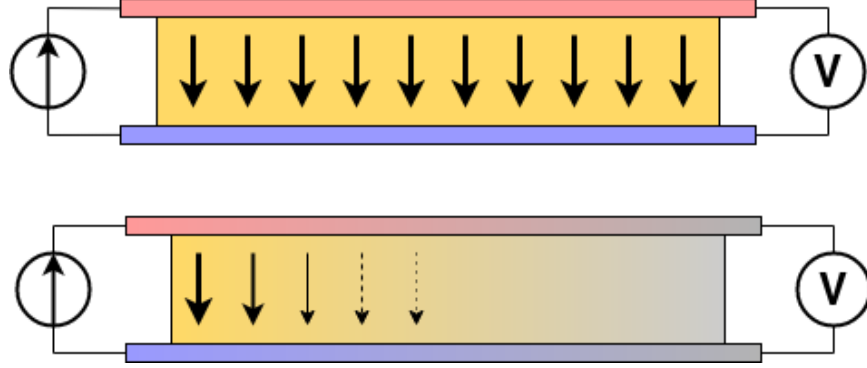


Figure 5: A comparison between contacting with ideally conducting electrodes (top) and electrodes with significant resistivity (bottom). Positive and negative voltages are shown as shades of red and blue in the electrodes, while the current density through the sample is depicted using arrows and shades of yellow. In the ideal case the contact voltages and current densities are uniform, while in the non-ideal case the current distribution is localized near the current injection point of the contacting electrodes.

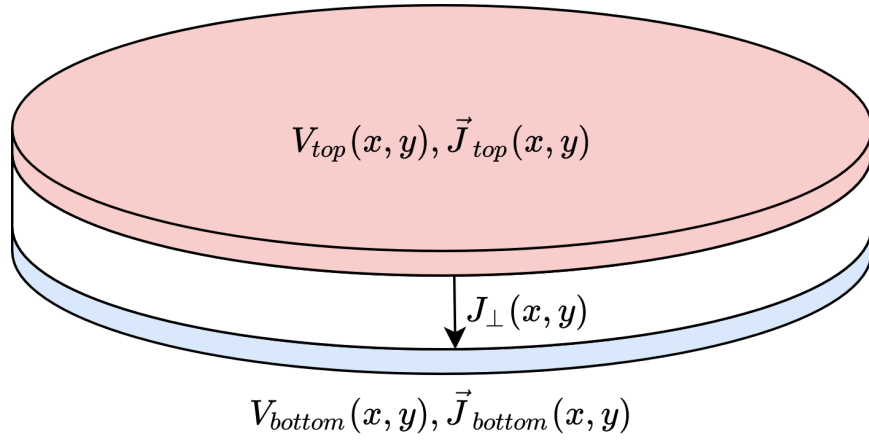


Figure 6: A model of a sample with two contacting electrodes. In the electrodes the current density is determined from the electrodes' conductivity and the electric fields. The current density through the sample can be determined from the stack resistivity  $\rho$  and the local potential difference between the top and bottom electrode.



and

$$\vec{J}_{bottom} = -\sigma \nabla_{(x,y)} V_{bottom}(x, y), \quad (5)$$

in which  $\sigma$  is the conductivity of the electrode material. The current density through the sample is given by

$$J_{\perp} = \frac{V_{top} - V_{bottom}}{\rho}, \quad (6)$$

for some specific sample resistance  $\rho$ . Consider charge conservation in some arbitrary region  $\Omega$  in the top electrode, which can be expressed as a sum of currents flowing into the region from other parts of the electrodes, and a current flowing into the sample:

$$0 = \int_{\Omega} \vec{J} \cdot d\vec{A} = \int_{\Omega} J_{\perp} dA + \oint_{\partial\Omega} \vec{J}_{top} \cdot \hat{n} h ds, \quad (7)$$

where  $h$  is the thickness of the electrode. Substitution of the current densities followed by application of the divergence theorem yields

$$0 = \int_{\Omega} \frac{1}{\rho} (V_{top} - V_{bottom}) dA - \int_{\Omega} \sigma h \nabla_{(x,y)}^2 V_{top} dA, \quad (8)$$

and similarly for the bottom equation, except the sign of the  $J_{\perp}$  contribution is switched

$$0 = \int_{\Omega} \frac{1}{\rho} (V_{top} - V_{bottom}) dA + \int_{\Omega} \sigma h \nabla_{(x,y)}^2 V_{bottom} dA. \quad (9)$$

Adding the two together, and letting  $\phi \equiv V_{top} - V_{bottom}$ , one gets

$$0 = \int_{\Omega} -\sigma h \nabla_{(x,y)}^2 \phi + \frac{\phi}{\rho} dA \quad (10)$$

As the choice of  $\Omega$  was arbitrary, the integrand must vanish almost everywhere, so that

$$\nabla^2 \phi = \frac{R_{sq}}{\rho} \phi. \quad (11)$$

No PDE is complete without appropriate boundary conditions, in this work Neumann boundary conditions are considered, as these describe four-point probing setups the best. A current distribution is driven along some part of the domain boundary, and some resulting potential difference is measured. In dimensionless form, the equation can be written as

$$\tilde{\nabla}^2 \phi = \left( \frac{L}{L_t} \right)^2 \phi \equiv k^2 \phi, \quad (12)$$

where  $L$  is the characteristic dimension of the sample, and  $L_t \equiv \sqrt{\frac{\rho}{R_{sq}}}$  is the so called transfer length, and the dimensionless Laplacian is given by  $\tilde{\nabla}^2 = \frac{1}{L^2} \nabla^2$ . In following sections the tilde on the Laplacian will be omitted, so that the dimensionless form of the PDE is given by

$$\nabla^2 \phi = k^2 \phi, \quad \Omega \quad (13)$$

$$\nabla \phi \cdot \hat{n} = f \quad \partial\Omega. \quad (14)$$

### 3.1.2 Uniqueness of solutions

To show that solutions are unique, consider two solutions,  $\phi_1$  and  $\phi_2$  and let  $\hat{\phi} \equiv \phi_1 - \phi_2$ , the goal will be to show that the PDE and boundary conditions force  $\phi$  to vanish. Linearity shows that  $\hat{\phi}$  must obey

$$\nabla^2 \hat{\phi} = k^2 \hat{\phi}, \quad \Omega \quad (15)$$

$$\nabla \hat{\phi} \cdot \hat{n} = 0 \quad \partial\Omega. \quad (16)$$

Now consider the following integral,

$$\int_{\Omega} \nabla \cdot (\hat{\phi} \nabla \hat{\phi}) dx = \oint_{\partial\Omega} \hat{\phi} \nabla \hat{\phi} \cdot d\vec{A} \stackrel{\text{B.C.}}{=} 0, \quad (17)$$

apply the chain rule

$$0 = \int_{\Omega} \nabla \cdot (\hat{\phi} \nabla \hat{\phi}) dx = \int_{\Omega} \hat{\phi} \nabla^2 \hat{\phi} + \nabla \hat{\phi} \cdot \nabla \hat{\phi} dx, \quad (18)$$

and apply the PDE to clear the  $\nabla^2 \hat{\phi}$  term,

$$0 = \int_{\Omega} k^2 \hat{\phi}^2 + |\nabla \hat{\phi}|^2 dx. \quad (19)$$

With the inner product

$$\langle \phi, \psi \rangle = \int_{\Omega} k \phi \psi + \nabla \phi \cdot \nabla \psi dx, \quad (20)$$

the result can be recognized as  $0 = \langle \hat{\phi}, \hat{\phi} \rangle \Rightarrow \hat{\phi} = 0$ , which proves that the solutions of the PDE are indeed unique.

### 3.1.3 Influence of transfer length

Now, let's solve these equations for a few geometries. The first is the simplest realizable geometry, take a sample, and contact it with pins at its center to drive the currents, while measuring a potential drop somewhere else along the sample. While in practice a rectangular sample is often used, the problem is reduced to a circular domain in order to more easily look into the spreading effects. The unit disk is chosen as a solution domain without the origin, at which the current is driven, by symmetry, this allows us to look at solutions of the form  $\phi(r)$ . As all currents are contained in the sample, the current density must vanish at the boundary, so that  $\phi'(1) = 0$ . In experimental conditions the total supplied current,  $I$ , is known. In this model however the average potential drop,  $\bar{\phi}$ , is specified, so that

$$\bar{\phi} = \frac{\int_{\Omega} \phi dA}{\int_{\Omega} dA} = \frac{2\pi}{\pi 1^2} \int_0^1 r \phi(r) dr. \quad (21)$$

In the adopted cylindrical coordinates, the PDE can be expressed as

$$r^2 \phi''(r) + r \phi'(r) - r^2 k^2 \phi(r) = 0, \quad (22)$$

which is known as the modified Bessel equation. This modified Bessel function has solutions:

$$\phi(r) = A I_0(kr) + B K_0(kr), \quad (23)$$

in which  $A$  and  $B$  are integration constants and  $I_0$  and  $K_0$  are modified Bessel functions of the first and second kind. By applying the boundary and integral conditions the integration constants can be found, these steps are omitted here, as it is mostly textbook linear algebra. In a simpler 1D system, the PDE reduces to  $\phi'' = k^2 \phi$ , which was solved with a similar boundary and integral condition. The solutions are shown in Figure 7

## 3.2 Idea: reduce effective sample dimensions

Suppose you were to conduct a four-point probing experiment in either geometry, in which a current is driven through the sample, and some potential difference between the top and bottom of the sample,  $\phi_M$ , is measured. What would be a good way to perform these measurements?

To answer this question, it is useful to first estimate  $L_t$  for the samples of interest. As the current distribution is least homogeneous for small  $L_t$ , it is safest to underestimate it by using large sheet resistivities and low stack resistivities. While the stack resistivity is of course not known before

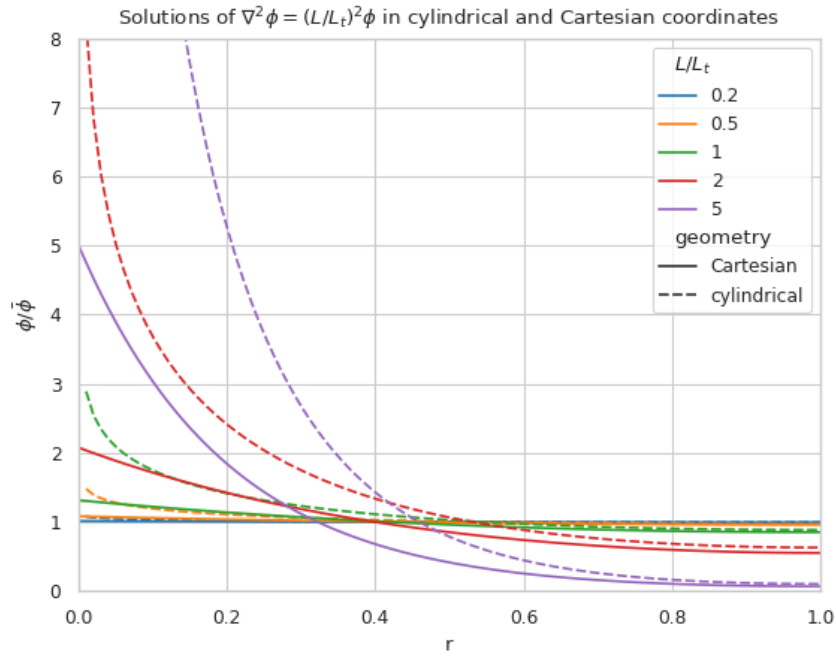


Figure 7: A comparison of solutions for  $\phi$  on  $(0, 1]$  in Cartesian and cylindrical coordinates, for varying  $k \equiv \frac{L}{L_t}$ . With boundary condition  $\phi'(1) = 0$  and integral condition  $\bar{\phi} = 1$ . Note that the cylindrical solutions have much steeper gradients than the Cartesian ones, and that the homogeneity of the current distribution depends strongly on  $k$ , with large  $k$  leading to very inhomogeneous currents.

the measurements, the lowest order of magnitude of  $\rho$  was estimated at  $10 \text{ m}\Omega\text{cm}^2$ , while for the used AZO films,  $R_{sq} \approx 100 \Omega$  is not uncommon, in this case the transfer length is on the order of  $0.1 \text{ mm}$ .

In practice, we'd like to be able to work with samples with dimensions of at least a few mm, not just because these are easier to handle, but because these can be easily be prepared by hand-cleaving a bigger sample piece. In these cases  $k$  would be significantly larger than 1, so the majority of current will be driven only through a small part of the sample near the current drive electrode.

The goal now is to reduce  $k$  through some means, in the ideal limiting case  $k = 0$ , but how close is close enough? In Figure 8, the normalized value of  $\phi$  is shown at the extremes of a sample for different  $k$ , the black horizontal line is at 99%. This shows that, in order to measure the average potential to within a percent relative error,  $k$  has to be around 0.25 or lower.

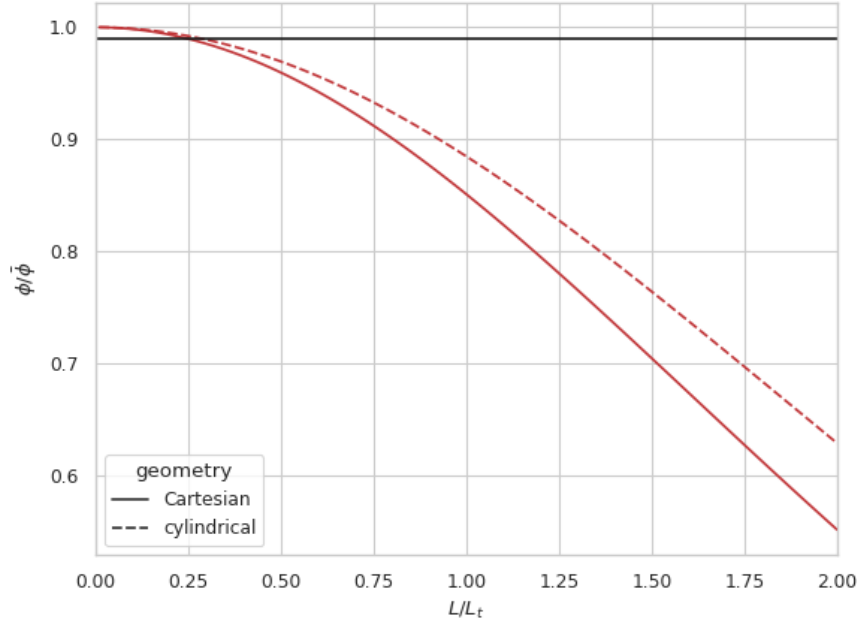


Figure 8:  $\frac{\phi_M}{\bar{\phi}}$  at the edge of the sample, as function of  $\frac{L}{L_t}$ . For small  $\frac{L}{L_t}$  the potential measured at the edge very closely resembles the average potential.

To realize this goal of decreasing  $\frac{L}{L_t}$ , two separate approaches are combined. The first is to increase  $L_t$  by making the contacting layers more

conductive, this is achieved by depositing 300nm of silver by e-beam evaporation. This increases  $L_t$  to approximately a few millimeters.

The second approach is to effectively reduce  $L$  by controlling the probe geometry. At first glance,  $L$  appears to be determined by the sample size, a current is driven through some point, and this current cannot flow out of the sample, represented in the boundary condition  $\phi'(L) = 0$ . An obvious option to reduce  $L$  could be to simply cut smaller samples, but in the millimeter range this is difficult, especially when areas need to be accurately determined. Working with tiny samples, while perfectly fine in theory, is undesired in practice, so can we decrease  $L$  in bigger samples? The answer is yes! The trick lies in the nature of the boundary condition, it is only required that  $\phi'(L) = 0$ , but does this imply that the sample is contained in the  $0 < x < L$  range? Not necessarily. As an example, consider the one dimensional case:  $\phi''(x) = k^2\phi(x)$  on  $(0, 1)$ . Now instead of applying a zero flux condition at any domain edge, simply consider solutions that are symmetric around  $x = \frac{1}{2}$ , these can easily be constructed from the solutions,  $\phi_k(x)$ , shown in Figure 8, by

$$\phi_{k,\text{sym}}(x) = \frac{1}{2}(\phi_k(x) + \phi_k(1 - x)). \quad (24)$$

Symmetric solutions are shown in Figure 9, it is clear that now  $\phi'(\frac{1}{2}) = 0$ . Notice the similarity between the solutions as shown in Figure 7 and the left half of Figure 9, they are the same! Apparently driving currents with a grid of symmetric electrodes will let us effectively change  $L$ .

### 3.2.1 TODOS

1. **TODO** Generalization to what? Weird wording, fix this

## 4 New approach

This approach was realized using custom made printed circuit boards (PCBs), as shown in Figure 10. The PCBs feature a pad of regularly spaced copper lines, covering an area of 15 by 15 mm<sup>2</sup>. The copper lines are alternately connected to either of the shown pins, so that they resemble interleaved combs. To perform a measurement, a sample is clamped between two such PCBs, and a current is driven between two combs on alternate sides of the sample, while the other combs are used to measure the resulting potential across the sample in a four-terminal configuration. The used copper lines were 0.6 mm wide and spaced 0.3 mm apart, with this spacing and a sample spreading

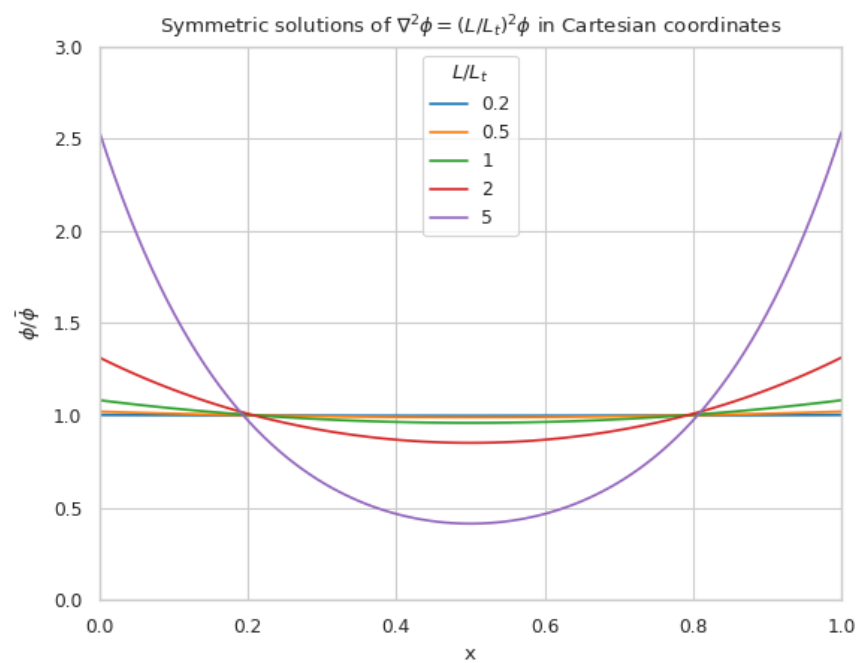


Figure 9: TODO

length on the order of half a cm, the requirement that  $\frac{L}{L_t} < 0.25$  is easily met, so that the current distribution can be considered homogeneous.

Practically, the measurements come down to the following steps:

1. Create samples that:
  - Have a spreading length significantly larger than the distance between the fingers of the PCBs to be used. Cover with silver if necessary.
  - Are homogeneous, this might not be the case when deposited films wrap around the samples.
  - Feature no edge deposited conductive films, it is recommended to cleave off the edges of the samples after silver deposition.
  - Have an accurately known surface area,  $A$ , in this work this was achieved with a computer vision method, which will be discussed later.
  - Fit on the 15 mm by 15 mm measurement pads of the PCBs.
2. Set up the resistance measurement system:
  - Use a sourcemeter in a four-terminal sensing configuration, in this work a Keithley 2400 was used.
  - Connect the current source terminals of the sourcemeter to “combs” on the two separate PCBs.
  - Connect the voltage measurement terminals to the remaining combs.
3. Clamp the sample between the PCBs
  - Make sure that the sample is located on the pads, and does not shift before measuring.
  - Use the alignment holes of the PCBs for consistent alignment.
  - Apply an evenly distributed pressure to the sample, this can be achieved with a glue clamp.
4. Perform a standard four-terminal resistance measurement, yielding resistance  $R$ .
5. Calculate the specific resistivity  $\rho_s = R \cdot A$ .



The interpretation of the measured stack resistivity depends on the used samples, as in this work symmetric samples were used, the stack resistivity must be larger than twice the interfacial resistivity of the AZO-Si interface. In this case an upper bound on contact resistivity can be given as  $\rho_c < \frac{1}{2}\rho_s$ .

## 5 Characterization of measurement method

So far the case for PCB measurements has boiled down on purely theoretical arguments, in the following chapters the measurement method will be experimentally characterized. The characterization will focus on two desired properties of the new measurement: reliability and validity. A measurement method is reliable when it is reproducible, yielding the same results on each measurement. Reliability by itself is not enough though, simply because observations being close to each other does not imply that they are close to the *correct* value. A measurement is called valid if its results actually resemble what is **intended** to be measured. For a good measurement system these two qualities obviously go hand in hand.

While the reliability often refers to repeated measurements under the exact same conditions, this strict definition is not very useful when considering the PCB measurements, as the goal is to reliably measure the contact resistivity **without** regard to some sample handling details. For context, the initial measurement system (TODO footnote: detail pin to plate) proved quite reliable when a single sample was contacted and stayed fixed between measurements. Problems started appearing however, as soon as this sample was contacted with different pins, in slightly different locations, rotated a bit, or a different sample piece was used. The estimated contact resistivities varied unpredictably when even slight, to the user practically unnoticeable, changes were made to the setup. The goal here is not to be reliable under strict control of all influencing factors, but to be reliable in a somewhat chaotic environment, one in which the user can choose not to care about the exact shape and contacting points of their samples, and still get *reliable* results. For this reason, the term reliability is used in a looser sense in this work: a measurement is considered reliable when it yields similar (enough) results in a range of realistic usage scenarios.

More practically speaking, these “realistic usage scenarios” should at least include different contacting conditions, like where the sample is located and in which orientation, but also simply using another sample of differing dimensions. These reliability experiments were done by varying exactly the mentioned conditions and measuring if these influence the measurement,

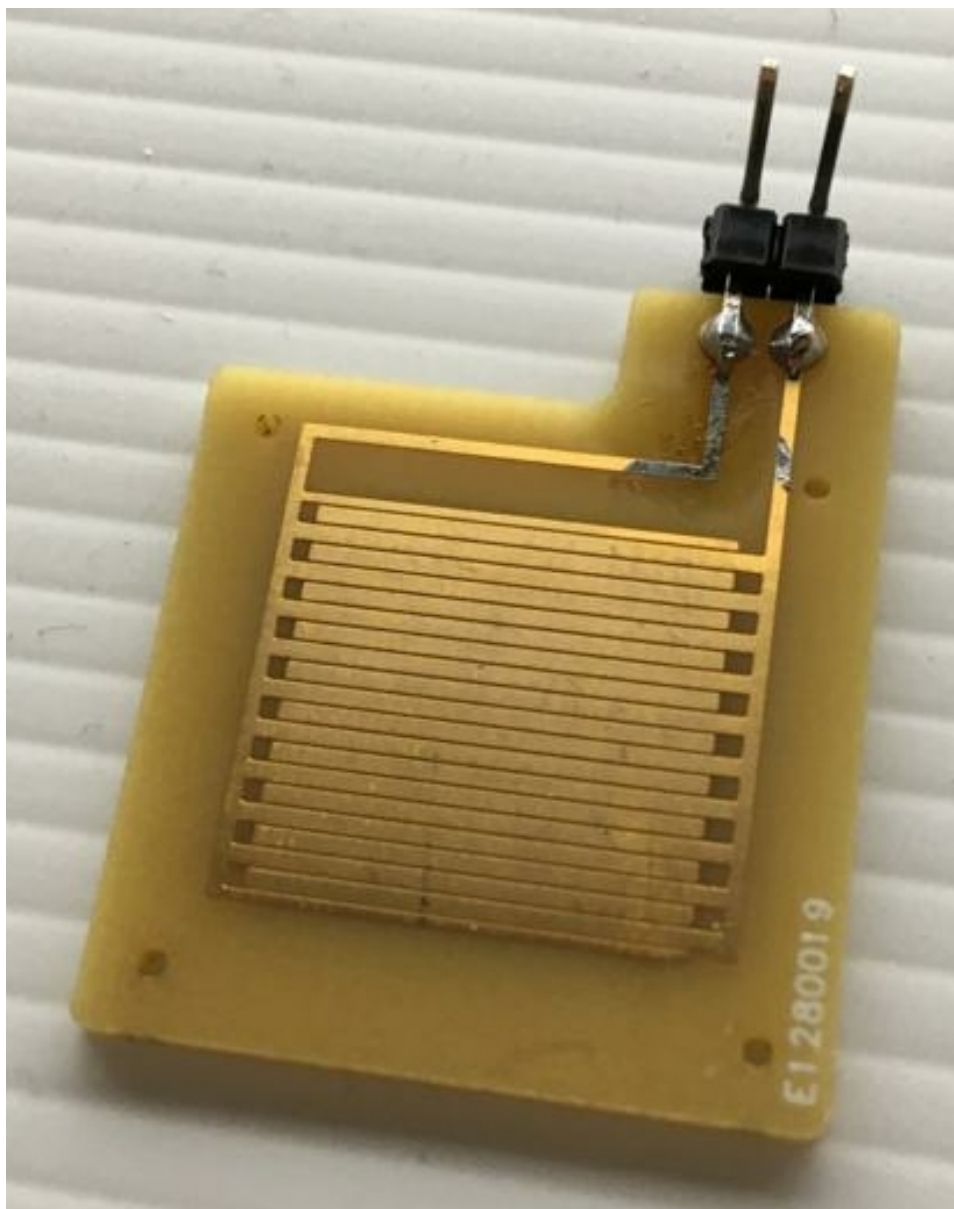


Figure 10: TODO

this will be discussed in more detail in following sections.

To check the validity of the measurement, a reference measurement is needed. Ideally a sample with a well known specific resistance could be used, but these were not available. Another option is to take a sample, measure the specific resistance through some other means, and then compare the results with the new method. This concurrent validity test was chosen, in which the novel method was compared to a cross bridge kelvin resistor (CBKR). The choice for a CBKR test was made since it can handle the same type of samples that the PCBs can. The needed patterning for Cox & Strack and other methods would imply the need to make separate samples, process them differently, and just hope that they have the same specific resistance. A CBKR allows for measurements on the exact same samples as on the PCBs, without any alterations, making it fit for a direct comparison of measurement methods.

## 5.1 TODOS

### 5.1.1 **DONE** Why check validity/reliability?

Because method has only been discussed theoretically, a proper assessment is needed in practice

1. **DONE** Contrast reliability validity Reliability indicates how closely the measurements are spaced. Validity indicates the error between measurement and actual value. Both are needed for a proper measurement. Reliability can be assessed using just the PCBs, for validity at least one secondary method is required for calibration.

### 5.1.2 **TODO** How will I check if the method works?

1. **TODO** Check reliability with PCBs As discussed before, the reliability can be assessed using just the PCBs, but how? Ideally this method is “hufter-proof”, in the sense that it doesn’t matter where the sample is exactly, as long as you know its area. First, the placement invariance is tackled in two steps: first the rotation (in?)variance, second the translation (in?)variance. After that, the sample area dependence is checked.
  - (a) **TODO** Is the measurement invariant in rotations? A few rectangular samples were selected (why these? basically arbitrary...) For these, measurements were conducted in either orientation, with the long side parallel to the fingers and with the short side

parallel to the fingers. To probe the per-measurement variance, measurements were conducted five times per orientation. (hint: does not matter much, you can mostly forget about it!)

- (b) **TODO** Is the measurement invariant in translations? Next, the influence of the position of the sample on measured  $\rho$  was checked. Here the samples were located at each extreme of the PCB, i.e. top-right, top-left, etc.. and in the center. This was done for a few samples, including those used in the rotation experiment, again multiple times.
  - (c) **TODO** Is the measurement invariant in sample area? Out of each sample wafer, different sample pieces were cut. A possible limitation of this method is that inhomogeneous processing such as localized backside deposition can effect in differences in overall sample resistivity. As it is difficult to cut out samples of specific sizes, wafer pieces are ranked by overall dimensions, with piece A being larger than piece B, and piece B being larger than piece C. These measurements were also performed on the five different positions noted in the translation invariance experiment, so that the resulting data can be used for either experiment.
2. **TODO** Check validity with CBKR While the reliability can be assessed using just the PCB method itself, an extra calibration is needed to assess the validity of the method. For this a Cross Bridge Kelvin Resistor setup was devised out of aluminium foil. A few samples were probed with the PCBs and the CBKR setup, measuring multiple times to obtain decent statistics. Ideally the results match for both measurement methods.
- (a) **TODO** How were CBKR experiments conducted? Cut out of aluminium foil.
  - (b) **TODO** Do the results match with the PCB method?

## 6 Results

### 6.1 Reliability

Ideally the PCB method should yield the same contact resistivities, regardless of

- Sample orientation,

- Sample position,
- Sample shape.

These assumptions were checked, starting with the sample orientation. Here the contact resistivity was measured for two cases, in the “long” case the long edge of the sample was aligned parallel to the fingers of the PCBs, while in the “short” case the short edge was aligned parallel to the fingers. This was done for two symmetric samples:

1. pSi substrate with r48 AZO annealed at 400C, measuring approx 4.5 mm by 6.5 mm.
2. 130  $\Omega$  n+ Si with r48 AZO annealed at 400C, measuring approx 6.5 mm by 9.0 mm.

The results are shown in Figure 11. For the pSi sample, the results are quite consistent, while for the n+ Si sample there is more spreading in the measurements. This can be explained by the pSi sample having a larger contact resistivity than the n+ Si sample, and thus a larger spreading length, this sample also happened to have smaller dimensions, so that overall the current distribution can be expected to be more homogeneous. Overall, the measurement seems most repeatable in the “short” configuration.

Next the location of the sample on the PCB was varied for a few samples. The samples were located at all four extreme corners of the PCB pad and at the center. Figure 12 shows the measured results for each of the tested samples, note the logarithmic vertical axis. This shows that the measurement is typically reliable on a per-sample basis. Clear are the deviations between pieces of similar samples, while these should all have the same contact resistivities, Figure 12 shows clear differences between samples which were cut out of exactly the same wafer.

### 6.1.1 TODOS

1. **TODD** Verschillen tussen samples Hoe komt dit? Deels backside depo, iig niet uit te sluiten, ervaring: backside depo goed weg snijden geeft vergelijkbare data. Deze dataset moet ik nog even goed bij elkaar sprokkelen. . .
2. **TODD** New samples with less backside depo Better results? -> Not really, dataset is small, no real way to know. . .

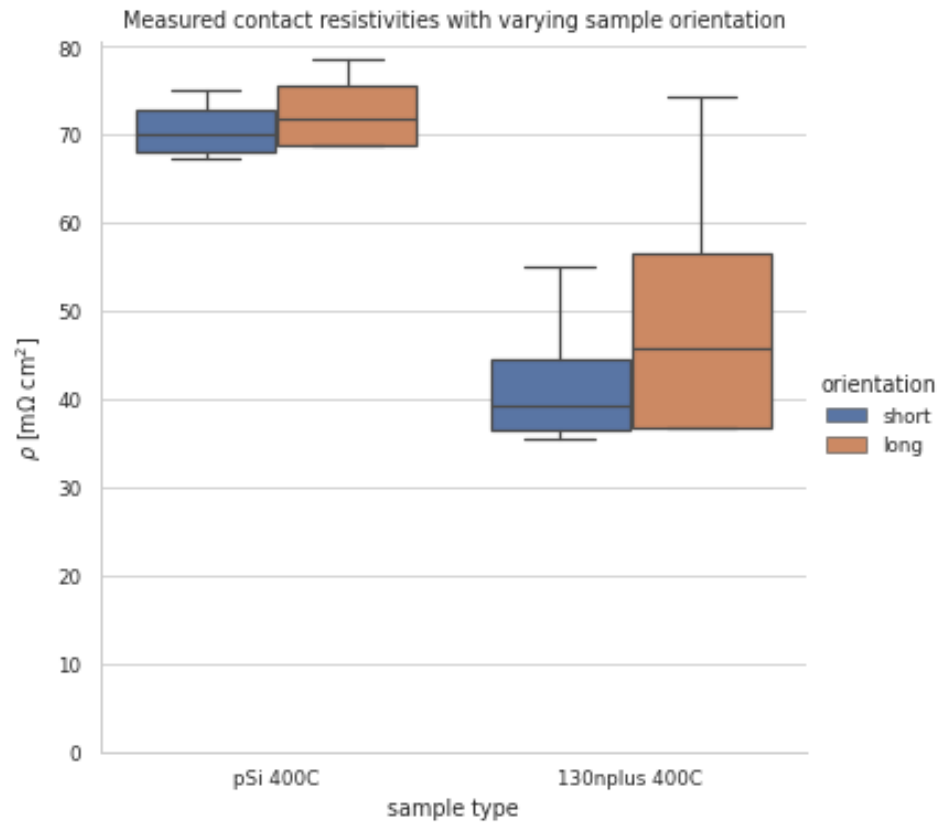


Figure 11: Measured contact resistivities with varying orientation. Two different samples were used, for which the contact resistivity was measured in different orientations. In the “short” cases, when the short side of the sample lies parallel to the PCB’s fingers, the measurements are most reliable.

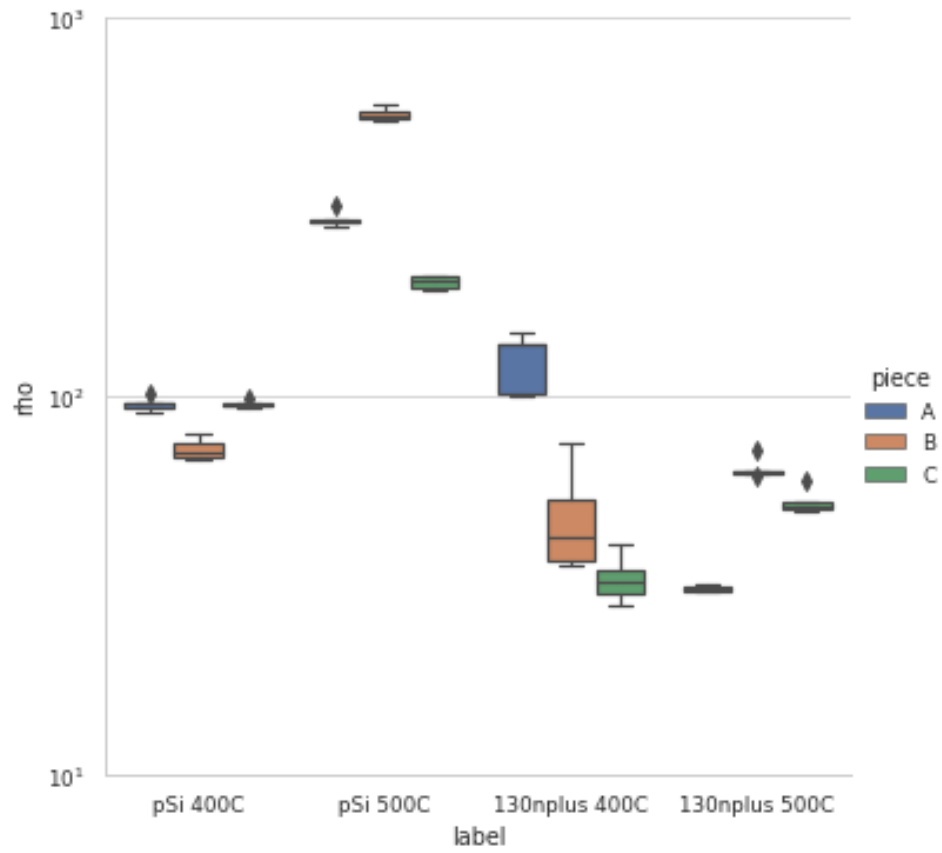


Figure 12: Measured contact resistivities of different pieces of different samples, the spread between measurements on different pieces are often larger than the spread within the pieces. This is not totally understood, but wrap-around of ALD films is expected to play a significant role.

## 6.2 Validity: Cross Bridge Kelvin Resistor comparison

Finally the PCB method was cross-validated with a Cross Bridge Kelvin Resistor (CBKR) setup which was carefully crafted from pieces of aluminium foil. While this alternate method is difficult and time consuming to perform, it provides a good sanity check for the PCB method. To do this, two L-shaped pieces of aluminium foil were cut, with the widths of the legs matching the dimensions of the samples. These contacting pads were made for each specific sample. Then the sample was clamped between the pieces of foil, while pieces of electrical tape ensured that no shorts could occur between the contacting pads. Two opposing “legs” were used to drive a current, while the potential difference was measured between the others, again in a four-point probe configuration. Several samples were used, for which the contact resistivity was measured multiple times with the PCB method and the CBKR method, Figure 13 shows that the results correlate strongly, here the error bars show the minimal and maximal values for each measurement.

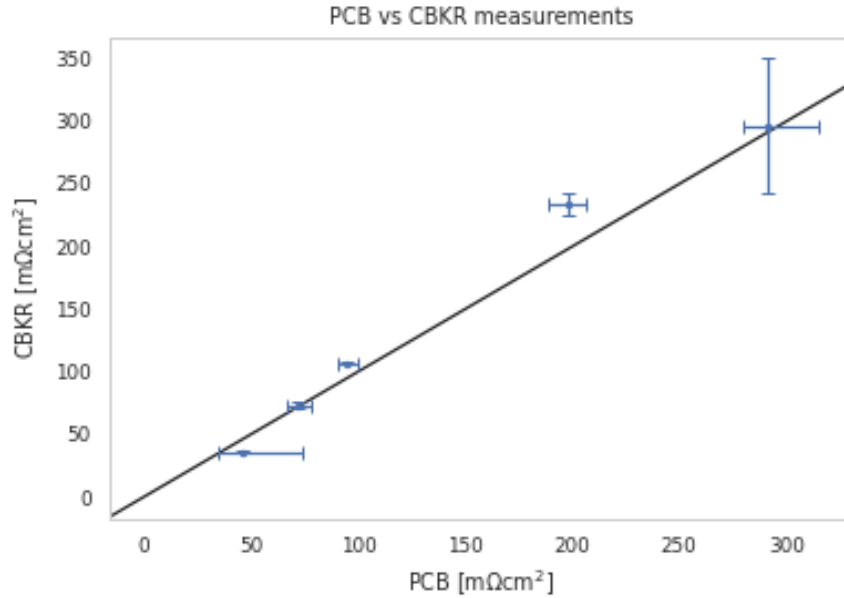


Figure 13: Comparison between PCB measurements and and CBKR measurements on a set of samples, the error bars indicate the minimum and maximum of the measured values. Ideally the measurements should match exactly, which is indicated by the black line.



## 7 Conclusion and outlook

A method for easy contact resistivity measurements was developed. In contrast to the Cox & Strack and transmission line methods, which involve delicate sample patterning steps, the method developed here only requires uniform conductive contacting layers.

### 7.1 TODOS

#### 7.1.1 TODO Ease of measurement

1. **TODO** Easy to execute
2. **TODO** Ag step still needed

#### 7.1.2 TODO Reliability of results

## 8 Conclusion

## 9 **TODO :noexport:**

### 9.1 **DONE** Waarde $L_t$ is ingeschat, wat betekent dit?

Met samples van  $1 \times 1 \text{ cm}^2$  betekent dit een flinke spreiding in mogelijke  $\phi_M$ , zeker in cilindrische samples (oftewel, naieve fpp setup). Wanneer je precies aan de rand meet is er een minder groot probleem, zie Figuur 8.

### 9.2 **DONE** Leuk, maar wat kunnen we hiermee?

Het zou mooi zijn als we  $L/L_t$  klein kunnen krijgen ( $\sim 0.25$  voor 1% error) zonder met ontzettend kleine ongecontroleerd gemaakte samples te hoeven werken. Vandaar: translatiesymmetrie, met een grid van electrodes breng je in principe dezelfde randvoorwaardes aan als in het originele cartesische geval (toelichting: symmetrie leidt tot  $\phi'(1) = 0$ ). Met hetzelfde sample kan je dus alsnog een veel kortere  $L$  bereiken.

### 9.3 **DONE** Implementatie: PCBs

Hoe zijn ze gemaakt, welke elektrische eigenschappen

### 9.4 **DONE** resultaten

Spreidingen laten zien, maken orientatie en sample grootte nog uit?

### **9.5 TODO Reflectie**

Methode vergelijkbaar met CBKR, ook in resultaten, in PCB setup lopen er echter geen stromen om het sample heen, wat een bron van fouten in CBKR weghaalt.

### **9.6 TODO Conclusie**

Methode is handig te gebruiken, levert herhaalbare resultaten.